Atmos. Chem. Phys. Discuss., 9, 27543–27569, 2009
www.atmos-chem-phys-discuss.net/9/27543/2009/

Atmospheric Chemistry and Physics Discussions

This discussion paper is/has been under review for the journal Atmospheric Chemistry and Physics (ACP). Please refer to the corresponding final paper in ACP if available.

Aerosol spectral absorption in the Mexico City area: results from airborne measurements during MILAGRO/INTEX B

R. W. Bergstrom[1], K. S. Schmidt[2], O. Coddington[2], P. Pilewskie[2], H. Guan[1], J. M. Livingston[3], J. Redemann[1], and P. B. Russell[4]

[1]Bay Area Environmental Research Institute, Sonoma, CA, USA
[2]Laboratory for Atmospheric and Space Physics, University of Colorado, Boulder, CO, USA
[3]SRI International, Menlo Park, CA, USA
[4]NASA Ames Research Center, Moffett Field, CA, USA

Received: 24 November 2009 – Accepted: 4 December 2009 – Published: 21 December 2009

Correspondence to: R. W. Bergstrom (bergstrom@baeri.org)

Published by Copernicus Publications on behalf of the European Geosciences Union.

Abstract

This paper presents estimates of the spectral solar absorption due to atmospheric aerosols during the 2006 MILAGRO/INTEX-B (Megacity Initiative-Local And Global Research Observations/Phase B of the Intercontinental Chemical Transport Experiment) field campaign. The aerosol absorption was derived from measurements of the spectral solar radiation and the spectral aerosol optical depth made on the J31 aircraft flying over the Gulf of Mexico and over Mexico City. We present the spectral single scattering albedo (SSA) and aerosol absorption optical depth (AAOD) for two flights over the Gulf of Mexico and three flights over Mexico City for wavelengths from 350 to approximately 1650 nm. The spectral aerosol optical properties of each case are different and illustrate the variability of the aerosol optical properties in the Mexico City area.

The results can be described in terms of three different wavelength region: The 350–500 nm region where the aerosol absorption often falls off sharply presumably due to organic carbonaceous particles and windblown dust; the 500–1000 nm region where the decrease with wavelength is slower presumably due to black carbon; and the near infrared spectral region (1000 nm to 1650 nm) where it is difficult to obtain reliable results since the aerosol absorption is relatively small and the gas absorption dominates. However, there is an indication of a small and somewhat wavelength independent absorption in the region beyond 1000 nm.

For one of the flights over the Gulf of Mexico near the coastline it appears that a cloud/fog formation and evaporation led to an increase of absorption possibly due to a water shell remaining on the particles after the cloud/fog had dissipated. For two of the Mexico City cases, the single scattering albedo is roughly constant between 350–500 nm consistent with other Mexico City results. In three of the cases a single absorption Angstrom exponent (AAE) fits the aerosol absorption optical depth over the entire wavelength range of 350 to 1650 nm relatively well (r^2>0.86).

1 Introduction

One of the largest climate uncertainties continues to be the radiative forcing due to atmospheric aerosols. A substantial fraction of that uncertainty is associated with the scattering and absorption of solar radiation by aerosols in cloud-free conditions, the so-called direct aerosol effect. In particular, the spectral absorption of solar radiation by atmospheric aerosols has been difficult to quantify. Use of an Angstrom Absorption Exponent (AAE, defined as the negative of the slope of a log-log plot of the aerosol absorption optical depth (AAOD) versus wavelength) has had some success in describing atmospheric aerosol absorption for certain aerosol types (Bergstrom et al., 2007). In general, black carbon (BC or light absorbing carbon, LAC) has an AAE near 1.0 while organic carbon (OC or organic matter OM) and dust have larger AAE's (Russell et al., 2009; Chen and Bond, 2009; Kirchstetter et al., 2004; and many others).

In recent years, a number of studies and field programs have aided in reducing the uncertainty of the direct aerosol radiative forcing (IPCC, 2007). MILAGRO/INTEX-B (Megacity Initiative-Local And Global Research Observations/Phase B of the Intercontinental Chemical Transport Experiment; Molina et al., 2009) was a recent field program conducted in the spring of 2006 where one of the goals was to study the aerosol radiative forcing in the Mexico City area. A compilation of papers is at ACP – Special Issue MILAGRO/INTEX-B 2006 (edited by: Molina, L. T., Madronich, S., Gaffney, J. S., Singh, H. B., and Pöschl, U.; http://www.atmos-chem-phys.org/special_issue83.html.)

This paper discusses the spectral aerosol absorption measured during the MILAGRO campaign in March 2006 and is one of a series of papers (Coddington et al., 2008; Livingston et al., 2009; Redemann et al., 2009; Schmidt et al., 2009) based on the data taken by the Solar Spectral Flux Radiometer (SSFR) and the 14 channel Ames Airborne Tracking Sunphotometer (AATS) instruments aboard the J31 aircraft. Coddington et al. (2008) presented results for the surface albedo in Mexico City and compared them with MODIS retrieved surface albedos. Livingston et al. (2009) compared the aerosol optical depth measurements measured by the AATS with satellite

retrievals. Redemann et al. (2009) compared J31 AATS measurements of AOD and related aerosol properties to results from MODIS-Aqua and MODIS-Terra, with emphasis on differences between the older MODIS Collection 4 (C4) and the new Collection 5 (C5) data set. Schmidt et al. (2009) present a new method of determining the aerosol radiative forcing and values for the aerosol radiative forcing above sea and land surfaces.

Mexico City is a very large urban area and has a wide array of aerosol sources producing particle types that can absorb solar radiation including wind-blown mineral dust, LAC or BC from biomass burning and transportation sources, and a significant amount of organic matter (OM). Previous studies have shown that the aerosol in the Mexico City atmosphere is a complex and highly variable mixture that presents a difficult challenge to the determination and interpretation of the aerosol optical properties (Barnard et al., 2008; Marley et al., 2009a, b; Corr et al., 2009; Adachi and Buseck, 2008; Shinozuka et al., 2009).

In this paper we use the term absorption to mean the amount of solar irradiance that is absorbed in a particular layer of the atmosphere. The fractional absorption is then the absorption divided by the solar irradiance incident on the top of the layer. The aerosol absorption optical depth (AAOD) of the layer is the aerosol extinction (absorption + scattering) optical depth (often termed just optical depth) multiplied by the co-albedo (which is 1 minus the single scattering albedo, SSA) of the layer.

2 Aircraft measurements

During MILAGRO in March 2006, the Jetstream 31 aircraft (J31) flew 13 missions from Veracruz, Mexico. The flights were either over the Gulf of Mexico or over the Mexico City area. The J31 daily mission summaries are at http://www.espo.nasa.gov/intex-b/flightplanningJ31.cgi and a table summarizing flights is in Molina et al. (2009). The SSFR and the AATS were mounted on the J31.

2.1 SSFR spectral solar radiant flux measurements

The SSFR is a moderate resolution (8–12 nm) spectrometer that spans the wavelength range from 350–2100 nm. The downward flux is corrected for the changing aircraft attitude with respect to the horizontal plane and for the angular response of the cosine-weighting integrating sphere (the optical collector for the SSFR). The cosine response is measured before each experiment in the laboratory to correct for non-linearities. The upward flux is corrected with the cosine-weighted response integrated over the lower hemisphere.

Pre- and post-mission, the SSFR is radiometrically calibrated against a NIST traceable 1000 W lamp. Field calibrations are performed to monitor the stability of the SSFR over the experiment using a 200 W LI-COR Field Calibrator. Spectral calibration is achieved by referencing lines from a Hg lamp. The SSFR RMS uncertainty is 3–5% over the SSFR spectral range. Both Coddington et al. (2008) and Schmidt et al. (2009) discuss the SSFR measurements of downwelling and upwelling solar irradiance made during the MILAGRO campaign.

2.2 AATS optical depth measurements

The AATS was also integrated on the J31 and measured aerosol optical depth (AOD) from flight level to the top of the atmosphere at 13 solar wavelengths (in the region of 354–2139 nm) and one wavelength for columnar water vapor (CWV) (Livingston et al., 2009). Vertical differentiation of AOD and CWV data obtained during J31 vertical profiles yields vertical profiles of multi-wavelength aerosol extinction and water vapor concentration, respectively. AOD uncertainties, calculated for each AATS data point, include four error sources: calibration, gas subtraction, detector output measurement, and airmass.

3 Analysis

The data from the SSFR and the AATS were combined and a radiative transfer model was used to determine the spectral aerosol absorption properties (Bergstrom, et al., 2003, 2004).

3.1 Radiative transfer model

Coddington et al. (2008) and Coddington (2009a) describe the recent improvements to a 1-D radiative transfer model (Bergstrom et al., 2003) designed for use in conjunction with the SSFR measurements. The major improvement is expanding the model from 140 bands of 10 nm width covering 300–1700 nm to 2201 bands of 1 nm sampling resolution that cover a wavelength range of 300–2500 nm. The model uses:

1. Correlated k-distributions for oxygen, ozone, carbon dioxide, water vapor, and methane for the molecular absorption coefficients.
2. Rayleigh optical depth for an atmosphere containing 370 ppm CO_2 calculated by numerical approximation.
3. DISORT (Discrete Ordinates Radiative Transfer Program).
4. Kurucz spectrum (Kurucz, 1995) at around 0.1 cm resolution for top of atmosphere (TOA) boundary condition.
5. SSFR slit functions.

The details of the absorption coefficient generation, sorting into distribution functions, the accounting for the spectral resolution of the instrument filter are described in Coddington et al. (2008, 2009b). The significant absorbing gas species (including overlapping species) in the spectral regions are listed in Table 2 of Coddington et al. (2008). For this study we added the NO2 absorption coefficients at each 1 nm band.

3.2 Flux divergence method

The flux divergence method to determine aerosol absorption can be described simply but is difficult to accomplish in practice. The net solar flux (downward minus upward) at the top and bottom of an aerosol layer are measured. The difference in the net solar flux is then the absorption in the layer (Chandrasekhar, 1960). There are many difficulties with this method, such as the horizontal inhomogeneity of the aerosol layer. In the Mexico City area it was not possible to fly completely below the Mexico City plume (due to flight restrictions) so that the plane flew at some distance above the surface inside the aerosol layer. Therefore the results are for the upper part of the urban plume.

4 Error and uncertainty analysis

4.0.1 Measurement uncertainty

The SSFR instrument accuracy is discussed in Coddington et al. (2008) and Schmidt et al. (2009) and the AATS instrument accuracy is discussed in e.g., Russell et al. (2007) and Livingston et al. (2009). Bergstrom et al. (2003) present the following equation for low surface albedo relating the error in the single scattering albedo, ω to the uncertainty in the fractional absorption (the absorption divided by the incident solar flux), α, and the extinction optical depth, τ:

$$\delta\omega=(1-\omega)\delta\alpha/\alpha+((\mu_o e^{-\tau/\mu_o})/(1-e^{-\tau/\mu_o}))\delta\tau \quad (1)$$

where μ_o is the cosine of the solar zenith angle. In general, the uncertainty estimates in the measured fractional absorption are about 0.01 (about 10% of the typical aerosol absorption in the shorter wavelengths) and the typical uncertainty in AATS-measured AOD is also ∼0.01. However, as the fractional absorption becomes small the uncertainty in the single scattering albedo becomes large.

4.0.2 Model uncertainty

Coddington et al. (2008) discuss the uncertainties in the new radiative transfer computer program. Since the flux divergence is only a weak function of the asymmetry factor (Bergstrom et al., 2003), we use the method to determine aerosol single scattering albedo (SSA). The AAOD is then just the aerosol optical depth times one minus the SSA.

In the region from 500 nm to 2000 nm errors in the amount of absorbing gases have an effect on the determination of the aerosol absorption properties. Figure 1a shows the absorption computed for 10 March case (discussed below) and the absorption computed for the same case with a 10% increase in the absorbing gases (H_2O, CO_2, O_3) amount. The difference in the absorption is difficult to see in Fig. 1a. However, Fig. 1b shows the percentage change in the absorption. Surprisingly, in the 500–2000 nm region there are very few wavelengths that are independent of the uncertainties in the absorbing gases. Even in the window regions between the water vapor bands, there is significant dependence on the gas amount, apparently related to the so-called continuum absorption of water vapor (where the strong lines of the absorption band influence the region between the bands) and the overlap of other gases. We computed the aerosol absorption properties only at the wavelengths shown in Fig. 1 to attempt to minimize the effect of uncertainties in the gas amounts. As a result the analysis had very narrow wavelength spacing (1 nm) in the 350 to 557 nm region and much larger spacing from 557 to 1622 nm. Another way to eliminate the effects of the gases is to solve for the gas amounts using all the wavelength information and minimize the least squared error between the measurements and predictions. We are exploring this approach and if possible will use it in the future.

For flights over Mexico City, the amount of O_3 and NO_2 are important inputs to the model (Barnard et al., 2008). For O_3 in the urban plume we estimated the values from the Ozone Monitoring Instrument (OMI) ozone column values. For NO_2 we used the OMI NO_2 column values as an estimate and then scaled the total column amount in

the same ratio as the aerosol optical depth assuming that all the NO_2 was in the urban plume.

In general, for aerosol optical depths greater than about 0.1 the uncertainty in the single scattering albedo is about 0.02. However, for low optical depths (particularly in the region beyond 1000 nm) the uncertainty in the single scattering albedo can be as high as 0.1. The uncertainty in AAOD is roughly 0.01 and in the region beyond 1000 nm, AAOD values are often below 0.01 making accurate estimates difficult.

5 Results

We present results from five separate flights, (2 flights over the Gulf of Mexico – 10 and 13 Marchand 3 flights over Mexico City – 6 March, 15 March and 19 March).

5.1 Gulf cases: 13 March and 10 March

For the Gulf cases the J31 flew from Veracruz up the coastline and then over the Gulf of Mexico corresponding to the location where viewing geometry was expected to be conducive to MODIS aerosol retrievals. Livingston et al. (2009) and Redemann et al. (2009) describe in some detail the flight plans of the J31 over the Gulf of Mexico.

The 13 March flight was a particularly interesting flight. Figure 2a and b show the GOES 12 satellite images before and during the flight with the flight path superimposed. Figure 2a shows the satellite image early in the morning where there was a cloud/fog bank over the region next to the coast where the flight path occurred later in the day. At the time of the flight, 4 h later, Fig. 2b shows that the cloud/fog had cleared and a residual part of it had moved somewhat further off shore. Starting at the location marked A the J31 flew at a low altitude over the water, then ascended through the residual cloud/fog, then descended to just above the water, and then continued in a northeasterly direction. At the location marked B the plane spiraled up and flew back toward the coast at an altitude of 5 km (above the aerosol layer). What appears in

Fig. 2b as a single line between A and B is actually two lines, one beneath the other representing the lower and upper passes.

SSFR and AATS data were obtained above and below the aerosol layer along the region between A and B. We hypothesize that the region from point A to the location of the cloud/fog remnant in Fig. 2b had been affected by the cloud/fog layer shown in Fig. 2a and that the region east of the cloud remnant in Fig. 2b was unaffected by the cloud. The layer average absorption, SSA and AAOD for the flight path west of the Fig. 2b cloud remnant and east of it are shown in Fig. 3a–d.

Figure 3a shows that there is slightly more absorption west of the Fig. 2b cloud remnant than east of that cloud. However, the single scattering albedo is higher west of the cloud than east of the cloud (Fig. 4b) meaning that there was relatively more scattering and higher optical depth for the aerosol that was previously in the cloud/fog of Fig. 2a. We hypothesize that this is due to water remaining on or in the aerosol droplets. Such a water coating would increase absorption coefficient (e.g., Redemann et al., 2001; Schwarz et al., 2008) in the flight path west of the Fig. 2b cloud remnant (as indeed was observed and is shown in Fig. 3c). The increase in absorption (about 30%) is consistent with recent results of Schwarz et al. (2008) for coated black carbon particles. Both the fact that the increase in scattering is larger than the increase in absorption and that the ratio of the two is a function of wavelength (shorter wavelengths are affected more than longer wavelengths) is also consistent with shell-core calculations (Bond et al., 2006; Redemann et al., 2001). Although there were no measurements of the amount of water actually on the aerosol particles, the results are interesting.

Fitting a straight line (constant AAE) to the entire spectrum shown in Fig. 3c does not do a good job of describing the absorption coefficient, particularly in the 350 nm region (r^2=0.74). The wavelength dependence of the absorption optical depth appears to be different within three distinct regions: 350 to roughly 500 nm, 500 to 1000 nm, and 1000 to 1700 nm. Figure 3d shows the AAE fit for the 300 to 500 nm region (r^2=0.96) and the 500 to 1000 nm (r^2=0.94). These r^2 values (also listed in Table 1) are notably larger than the r^2 of 0.74 obtained for a single-AAE fit for the entire wavelength range,

indicating a much better fit. The spectral AAOD behavior shown in Fig. 3 is similar to many recent results where the aerosol is composed of OM and BC (e.g., Martins et al., 2009; Barnard et al., 2008) where the AAE is larger in the UV region and then near 1.0 in the visible to near IR region. As shown in Table 1, the extinction Angstrom exponents for this day were 1.0 and 0.8 west and east, respectively, of the remnant cloud in Fig. 2b, indicating relatively large particles (i.e., dust) so that the aerosol is perhaps a mixture of dust, OM and BC.

The results for the other Gulf case (10 March) are shown in Fig. 4a and b and Table 1. The SSA increases with wavelength and a single AAE fit is relatively good with value of 2.6 (r^2=0.89). However, the AAOD values between 1200 and 1600 nm are significantly less than 0.01 and exhibit a large spread. The extinction Angstrom exponent for this day was 0.8 indicating fairly large particles.

Comparing the 13 March case with the March 10th case shows the difficulty in making generalizations about the atmospheric aerosol given only a few cases. In the 13 March case the SSA generally decreases with wavelength while for the 10 March case the SSA increases with wavelength. In the 13 March case the AAE is not constant with wavelength while for the 10 March case the AAE is relatively constant with wavelength.

Both Figs. 3c and 4b show an absorption feature at 480 nm. This appears to be a water vapor band that is not well characterized by the model.

5.2 Mexico City area cases: 6 March, 15 March and 19 March

We estimated the aerosol spectral absorption and absorption optical depth values for three days when the plane flew over the Mexico City area, 6 March, 15 March and 19 March. Each day's results are somewhat different.

To show the variation in absorption with the thickness of the layer above the plane, the fractional spectral absorption for 6 March is shown in Fig. 5 for passes at three different heights (250, 550, and 1850 m above the surface). As the plane flew closer to the surface the absorption due to both aerosol and water vapor increased. However,

the fractional absorption due to water vapor over Mexico City (Fig. 5) is less than that over the Gulf (Fig. 3a) since, at 2240 m above sea level, there is less water vapor in the Mexico City atmosphere and also because the plane was well above the surface.

The SSA and AAOD for the three cases over Mexico City are shown in Fig. 6a–f. The 6 March results are for a flight above the urban center (T0) at two different altitudes (250 and 550 m above the surface). Figure 6a shows the SSA is relatively constant or even decreases between 350 and 500 nm then increases after 500 nm. This spectral behavior is similar to other results for Mexico City reported by Barnard et al. (2008), Marley et al. (2009b) and Corr et al. (2009), who point to absorption by organic material as the most likely explanation. (Another possibility is dust combined with BC; Jeong and Sokolik, 2008.) The error bars are quite large for wavelengths greater than 700 nm since the optical depth was relatively small as the plane was in the upper part of the urban plume.

The aerosol absorption optical depths in Fig. 6b also show a change in slope at about 500 nm with a steeper slope for wavelengths >500 nm. The absorption optical depth past 1000 nm is below 0.01 and somewhat constant. In spite of the aforementioned slope change, a constant AAE fits the spectrum relatively well (AAE=2.2, r^2=0.97; and AAE=1.9, r^2=0.97).

The 15 March case in Fig. 6c and d is also for a flight 250 m over T0, and the results are similar to the 6 March case in that the SSA is relatively constant from 350 to 500 nm. However, the SSA in this case is larger and decreases at wavelengths >700 nm, but again with large error bars at those wavelengths. The aerosol absorption optical depth falls off at a relatively constant slope between 350 and 1000 nm. The AAE value is 1.4, which is somewhat larger than expected from BC only suggesting that the aerosol is mostly BC with some OM.

The 19 March flight was interesting and is discussed in detail in Livingston et al. (2009). The winds over Mexico City were quite strong and resulted in a large amount of windblown dust, particularly at T2 (a rural area 63 km northeast of T0). The visibility near T2 was very poor and the plane flew at about 420 m above ground level (a.g.l.)

near T2. The atmosphere was somewhat clearer at T0 (it was a Sunday) and the plane flew at 600 m near T0. Despite the difference in altitude the optical depths above the plane for the two cases were similar (Livingston et al., 2009). The SSA and AAOD results are shown in Fig. 6e and f. For both the T0 and T2 results the SSA increases between 350 and 500 nm and then is fairly constant. The AAOD decreases rapidly between 350 nm and about 700 nm and the AAE for T2 is larger than T0 indicating perhaps the effect of BC combining with the dust in the urban center at T0. The difference in the magnitude of the AAOD is due to the smaller SSA (more absorption) at T0 as compared to T2.

5.3 Summary of the results

The results for the AAE for 350–500 nm and 500–1000 nm, the increase or decrease of SSA with wavelength, and the extinction Angstrom exponent (EAE) are shown in Table 1. Looking at Table 1, one can easily identify the 19 March dust case by the very small EAE values. The EAE of 0.0 represents very large particles [and the flattest extinction spectrum seen by the AATS researchers in many years of making measurements]. The fact that this dust case has the largest AAE values for 350–500 nm is consistent with the results of Bergstrom et al. (2007) and Russell et al. (2009). For the 19 March case the constant AAE extends to 600 nm indicating that a division at 500 nm is simply an approximation.

6 Discussion and comparison to other results

6.1 Mexico City results

As mentioned above, previous studies of the aerosol radiative properties in the Mexico City area (Barnard et al., 2008; Marley et al., 2009a, b; Corr et al., 2009) report enhanced absorption in the 300–500 nm wavelength range. Corr et al. (2009) find SSA

having little or no wavelength dependence for the wavelength pair 332 and 368 nm, with values varying between ∼0.70 and ∼0.86. Barnard et al. (2008) also find SSA having little or no wavelength dependence between ∼300 and ∼400 nm, with values varying between ∼0.67 and ∼0.78. Barnard et al. (2008) report a steep increase in SSA between ∼400 and 500 nm, with SSA(500 nm) ∼0.87 to 0.95, and decreasing SSA from 500 to 870 nm, with SSA(870 nm) ∼0.81 to ∼0.93. They attribute the enhanced absorption for λ<400 nm to organic matter, as do Marley et al. (2009a, b).

Barnard et al. (2008) find AAE values that are strongly dependent on wavelength pair (3.2 to 5.1 for 300–500 nm; 1.9 to 2.6 for 300–870 nm). Marley et al. (2009b) find a range of AAE (0.63 to 1.5 including data from an earlier campaign in 2003 and the 2006 results) over the wavelength range 370 to 950 nm. It should be noted that most of the data used by Barnard et al. (2008) was from 2003 when there were forest fires in the Yucatan giving more OM sources than during 2006 (Marley et al., 2009b).

Our results compare reasonably well with the other results in that the SSA over Mexico City is constant in the 350–400 nm range. We do not see the sharp increase between 400 and 500 nm seen by Barnard et al. (2008). However, this difference could be due to the increased forest fires in 2003. Our AAE values have a similar range as Barnard et al. (2008) but a larger range than Marley et al. (2009b). For the 15 March case, our AAE results agree well with Marley et al.'s results (0.96 compared with 0.93 afternoon average).

6.2 Other recent results

The idea that individual aerosol components have a unique AAE opens up the possibility of determining the amount of the absorbing species. Recently, Yang et al. (2009) used the wavelength dependence of various aerosol components to apportion the aerosol absorption in Northern China for black carbon, brown carbon (OM), and dust, attributing the high AAE values of dust to the presence of ferric oxides. In one of the MILAGRO studies discussed above, Barnard et al. (2008) subtracted a BC-type (AAE=1) absorption from the total absorption and attributed the remainder to OM. Martins et

al. (2009) compared the results for two urban areas, Sao Paulo, Brazil and Greenbelt, Maryland. They showed that Sao Paulo had increased shortwave absorption presumably due to organics.

Another method of analyzing absorption data is to plot the absorption data with the AAE on one axis and the EAE on the other axis. This has been used by a number of investigators recently (Yang et al., 2009; Fig. 5 and Russell et al., 2009; Fig. 5). Shinozuka et al. (2009) plotted AAE versus the organic mass fraction and SSA while Mielonen et al. (2009) categorized the aerosol by SSA and EAE. These techniques rely on the idea that BC, OM and dust have different locations on the figures. Plots of the data do tend to group in this manner, however there is a large amount of scatter and some of the groups overlap (see Yang et al., 2009; Fig. 5). Yang et al. (2009) identified the specific aerosol type by doing a back trajectory to source locations.

It is difficult to compare our single case results with average values over many cases (Yang et al., 2009) or long-term averages (Russell et al., 2009). However, their results can be compared for our dust case (19 March). Yang et al. (2009) have an average of the dust cases at AAE=1.89 and EAE=0.59. Russell et al. (2009) have multi-year AERONET-derived averages over three desert dust-influenced sites of AAE=2.2 and EAE=0.6. Our dust case has a larger AAE values (3.3 for T2 350–500 nm) and smaller EAE values (0.0 for T2) than the average values but are within the ranges seen by both other studies.

The other cases are more problematic to compare. Yang et al. (2009) have the averages of AAE and EAE for biomass burning, fresh plume and coal pollution with very similar values (1.5 and 1.5; 1.35 and 1.49; and 1.46 and 1.39). Similarly the Russell et al. (2009) multi-year AERONET averages are 1.3 and 1.9 for biomass burning and 1.0 and 1.8 for urban pollution. Our non-dust results range from an AAE of 0.96 to 3.3 and an EAE of 0.7 to 1.8. In general then, while our results fit into the range of values seen by other investigators, it is difficult to identify the source of the absorbing material (other than dust) from an AAE versus EAE plot (or the SSA trend with wavelength) without more information.

7 Conclusions

The results for the spectral single scattering albedo and absorption optical depth for the Mexico City area show a great deal of variability most likely due to aerosol mixtures of varying amounts of organic carbon, black carbon and dust. The aerosol spectral absorption optical depth appears to generally fall into three different wavelength regions:

- 300–500 nm region where AAOD often falls off sharply towards longer wavelengths due to organic carbonaceous particles and windblown dust;
- 500–1000 nm region where the AAOD decrease with wavelength is slower most likely due to black carbon; and
- 1000 nm to 2000 nm where it was difficult for us to obtain reliable results since the AAOD was relatively small and the gas absorption dominated. However, there was an indication of a small and somewhat wavelength independent absorption in this region.

Of the five cases, two had a single, constant absorption Angstrom exponent (AAE) that fit the absorption optical depth over the entire wavelength range of 350 to 1700 nm. The other three cases required separate fits for the 350 to 500 nm and 500 to 1000 nm region.

Acknowledgements. All of the authors were supported by the NASA Radiation Science Program, under the direction of Hal Maring. RWB and HG were supported by NASA Grant NNX08AH60. KSS, OC and PP were supported by NASA Grant NNX08AI83G.

References

Adachi, K. and Buseck, P. R.: Internally mixed soot, sulfates, and organic matter in aerosol particles from Mexico City, Atmos. Chem. Phys., 8, 6469–6481, 2008, http://www.atmos-chem-phys.net/8/6469/2008/.

Barnard, J. C., Volkamer, R., and Kassianov, E. I.: Estimation of the mass absorption cross section of the organic carbon component of aerosols in the Mexico City Metropolitan Area, Atmos. Chem. Phys., 8, 6665–6679, 2008, http://www.atmos-chem-phys.net/8/6665/2008/.

Bergstrom, R. W., Pilewskie, P., Schmid, B., and Russell, P. B.: Estimates of the spectral aerosol single scattering albedo and aerosol radiative effects during SAFARI 2000, J. Geophys. Res., 108(D13), 8474, doi:10.1029/2002JD002435, 2003.

Bergstrom, R. W., Pilewskie, P., Pommier, J., Rabbette, M., Russell, P. B., Schmid, B., Redemann, J., Higurashi, A., Nakajima, T., and Quinn, P. K.: Spectral absorption of solar radiation by aerosols during ACE-Asia, J. Geophys. Res., 109, D19S15, doi:10.1029/2003JD004467, 2004.

Bergstrom, R. W., Pilewskie, P., Russell, P. B., Redemann, J., Bond, T. C., Quinn, P. K., and Sierau, B.: Spectral absorption properties of atmospheric aerosols, Atmos. Chem. Phys., 7, 5937–5943, 2007, http://www.atmos-chem-phys.net/7/5937/2007/.

Bond, T. C., Habib, G., and Bergstrom, R. W.: Limitations in the enhancement of visible light absorption due to mixing state, J. Geophys. Res., 111, D20211, doi:10.1029/2006JD007315, 2006.

Chandrasekhar, S.: Radiative Transfer, New York: Dover, 393 p., 1960.

Chen, Y. and Bond, T. C.: Light absorption by organic carbon from wood combustion, Atmos. Chem. Phys. Discuss., 9, 20471–20513, 2009, http://www.atmos-chem-phys-discuss.net/9/20471/2009/.

Coddington, O., Schmidt, K. S., Pilewskie, P., Gore, W. J., Bergstrom, R. W., Román, M. O., Redemann, J., Russell, P. B., Liu, J., and Schaaf, C. B.: Examining the impact of overlying aerosols on the retrieval of cloud optical properties from passive remote sensing, J. Geophys. Res., doi:10.1029/2008JD010089, accepted on 14 December 2009, 2008.

Coddington, O.: The application of airborne shortwave spectral irradiance measurements to atmosphere and surface remote sensing, Phd Thesis, University of Colorado, 2009a.

Coddington, O., Schmidt, K. S., Pilewskie, P., Gore, W. J., Bergstrom, R. W., Román, M., Redemann, J., Russell, P. B., Liu, J., and Schaaf, C. C.: Aircraft measurements of spectral surface albedo and its consistency with ground-based and space-borne observations, J. Geophys. Res., 113, D17209, doi:10.1029/2008JD010089, 2008.

Corr, C. A., Krotkov, N., Madronich, S., Slusser, J. R., Holben, B., Gao, W., Flynn, J., Lefer, B., and Kreidenweis, S. M.: Retrieval of aerosol single scattering albedo at ultraviolet wavelengths at the T1 site during MILAGRO, Atmos. Chem. Phys., 9, 5813–5827, 2009, http://www.atmos-chem-phys.net/9/5813/2009/.

IPCC, 2007: Climate Change 2007: The Physical Science Basis, Contribution of Working Group I to the Fourth Assessment Report of the Intergovernmental Panel on Climate Change, edited by: Solomon, S., Qin, D., Manning, M., Chen, Z., Marquis, M., Averyt, K. B., Tignor, M., and Miller, H. L., Cambridge University Press, Cambridge, UK and New York, NY, USA, 2007.

Jeong, G. N. and Sokolik, I. N.: Effect of mineral dust aerosols on the photolysis rates in the clean and polluted marine environments, J. Geophys. Res., 112, D21308, doi:10.1029/2007JD008442, 2007.

Kirchstetter, T. W., Novakov, T., and Hobbs, P.: Evidence that the spectral dependence of light absorption by aerosols is affected by organic carbon, J. Geophys. Res., 109, D21208, doi:10.1029/2004JD004999, 2004.

Kurucz, R. L.: The solar spectrum: atlases and line identifications. Presented at the Workshop on Laboratory and Astronomical High Resolution Spectra, 29 August–2 September 1994, Brussels, in: Laboratory and Astronomical High Resolution Spectra, Astron. Soc. of the Pacific Conf. Series 81, edited by: Sauval, A. J., Blomme, R., and Grevesse, N., San Francisco, Astron. Soc. of the Pacific, 17–31 pp., 1995.

Livingston, J. M., Redemann, J., Russell, P. B., Torres, O., Veihelmann, B., Veefkind, P., Braak, R., Smirnov, A., Remer, L., Bergstrom, R. W., Coddington, O., Schmidt, K. S., Pilewskie, P., Johnson, R., and Zhang, Q.: Comparison of aerosol optical depths from the Ozone Monitoring Instrument (OMI) on Aura with results from airborne sunphotometry, other space and ground measurements during MILAGRO/INTEX-B, Atmos. Chem. Phys., 9, 6743–6765, 2009, http://www.atmos-chem-phys.net/9/6743/2009/.

Marley, N. A., Gaffney, J. S., Castro, T., Salcido, A., and Frederick, J.: Measurements of aerosol absorption and scattering in the Mexico City Metropolitan Area during the MILAGRO field

campaign: a comparison of results from the T0 and T1 sites, Atmos. Chem. Phys., 9, 189–206, 2009,
http://www.atmos-chem-phys.net/9/189/2009/.

Marley, N. A., Gaffney, J. S., Tackett, M., Sturchio, N. C., Heraty, L., Martinez, N., Hardy, K. D., Marchany-Rivera, A., Guilderson, T., MacMillan, A., and Steelman, K.: The impact of biogenic carbon sources on aerosol absorption in Mexico City, Atmos. Chem. Phys., 9, 1537–1549, 2009,
http://www.atmos-chem-phys.net/9/1537/2009/.

Martins, J. V., Artaxo, P., Kaufman, Y. J., Castanho, A. D., and Remer, L. A.: Spectral absorption properties of aerosol particles from 350–2500 nm, Geophys. Res. Lett., 36, L13810, doi:10.1029/2009GL037435, 2009.

Mielonen, T., Arola, A., Komppula, M., Kukkonen, J., Koskinen, J., de Leeuw, G., and Lehtinen, K. E. J.: Comparison of CALIOP level 2 aerosol subtypes to aerosol types derived from AERONET inversion data, Geophys. Res. Lett., 36, L18804, doi:10.1029/2009GL039609, 2009.

Molina, L. T., Madronich, S., Gaffney, J., et al.: An Overview of MILAGRO 2006 Campaign: Mexico City Emissions and its Transport and Transformation, submitted to Atmos. Chem. Phys. Discuss., 2009.

Redemann, J., Russell, P. B., and Hamill, P.: Dependence of aerosol light absorption and single scattering albedo on ambient relative humidity for sulfate aerosols with black carbon cores, J. Geophys. Res., 106, 27485–27495, 2001.

Redemann, J., Zhang, Q., Livingston, J., Russell, P., Shinozuka, Y., Clarke, A., Johnson, R., and Levy, R.: Testing aerosol properties in MODIS Collection 4 and 5 using airborne sunphotometer observations in INTEX-B/MILAGRO, Atmos. Chem. Phys., 9, 8159–8172, 2009, http://www.atmos-chem-phys.net/9/8159/2009/.

Russell, P. B., Livingston, J. M., Redemann, J., Schmid, B., Ramirez, S. A., Eilers, J., Khan, R., Chu, A., Remer, L., Quinn, P. K., Rood, M. J., and Wang, W.: Multi-Grid-Cell Validation of Satellite Aerosol Property Retrievals in INTEX/ITCT/ICARTT 2004, J. Geophys. Res., 112, D12S09, doi:10.1029/2006JD007606, 2007.

Russell, P. B., Bergstrom, R. W., Shinozuka, Y., Clarke, A. D., DeCarlo, P. F., Jimenez, J. L., Livingston, J. M., Redemann, J., Holben, B., Dubovik, O., and Strawa, A.: Absorption Angstrom Exponent in AERONET and related data as an indicator of aerosol composition, Atmos. Chem. Phys. Discuss., 9, 21785–21817, 2009,

http://www.atmos-chem-phys-discuss.net/9/21785/2009/.

Schmidt, K. S., Pilewskie, P., Bergstrom, R., Bierwirth, E., Coddington, O., Redemann, J., Livingston, J., Russel, P., Wendisch, M., and Gore, W.: Aerosol radiative properties from airborne measurements over ocean and land during MILAGRO, in preparation, 2009.

Schwarz, J. P., Spackman, J. R., Fahey, D. W., et al.: Coatings and their enhancement of black carbon light absorption in the tropical atmosphere, J. Geophys. Res., 113, D03203, doi:10.1029/2007JD009042, 2008.

Shinozuka, Y., Clarke, A. D., DeCarlo, P. F., Jimenez, J. L., Dunlea, E. J., Roberts, G. C., Tomlinson, J. M., Collins, D. R., Howell, S. G., Kapustin, V. N., McNaughton, C. S., and Zhou, J.: Aerosol optical properties relevant to regional remote sensing of CCN activity and links to their organic mass fraction: airborne observations over Central Mexico and the US West Coast during MILAGRO/INTEX-B, Atmos. Chem. Phys., 9, 6727–6742, 2009,
http://www.atmos-chem-phys.net/9/6727/2009/.

Yang, M., Howell, S. G., Zhuang, J., and Huebert, B. J.: Attribution of aerosol light absorption to black carbon, brown carbon, and dust in China - interpretations of atmospheric measurements during EAST-AIRE, Atmos. Chem. Phys., 9, 2035–2050, 2009,
http://www.atmos-chem-phys.net/9/2035/2009/.

Table 1. Retrieved aerosol optical properties.

Date	AAE 350–500 nm	AAE 500-1000 nm	SSA	EAE*
Gulf cases				
13 March				
West**	1.8 (r^2=0.96)	1.1 (r^2=0.94)	decrease	1.4
East**	1.4 (r^2=0.88)	0.8 (r^2=0.90)	decrease	1.1
10 March	2.6 (r^2=0.89)		increase	1.6
Mexico City cases				
6 March				
250 m T0	1.7 (r^2=0.98)	3.1 (r^2=0.96)	increase	1.9
540 m T0	1.4 (r^2=0.99)	2.3 (r^2=0.93)	increase	1.7
15 March	0.96 (r^2=0.86)		decrease	1.1
19 March				
T0	2.2 (r^2=0.99)	0.7 (r^2=0.48)	increase	0.3
T2	3.3 (r^2=0.98)	4.4 (r^2=0.42)	increase	0.0

* EAE calculated from 450 to 800 nm to be consistent with Yang et al. (2009) and Russell et al. (2009). (AERONET-derived EAE values for 440 and 870 nm)
* Portion of flight path relative to cloud/fog remnant in Fig. 2b.

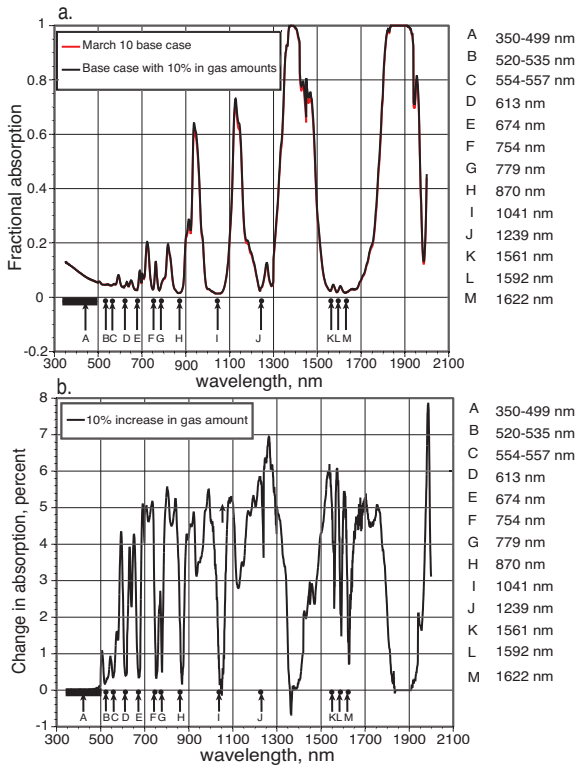

Fig. 1. **(a)** Fractional absorption for the 6 March case. **(b)** Percentage change in fractional absorption for a 10% increase in gas amounts.

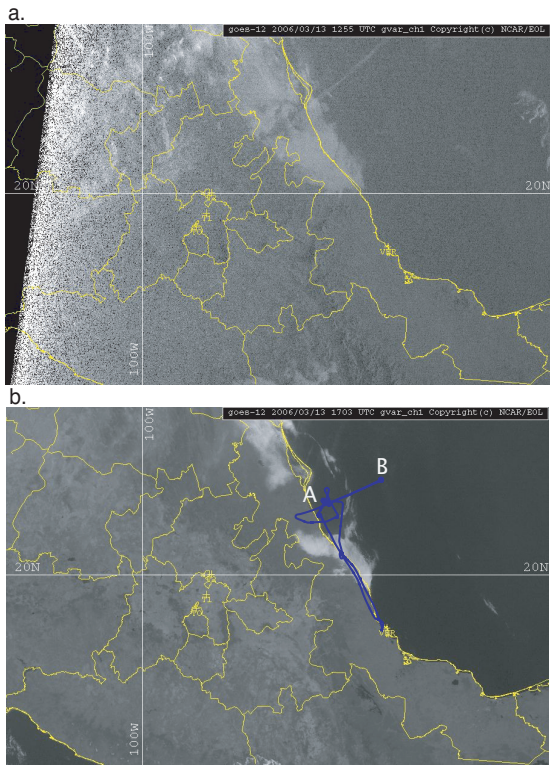

Fig. 2. **(a)** GOES 16 satellite image on 13 March 2006 at 12:55 UTC. **(b)** GOES 16 satellite image on 13 March 2006 at 17:03 UTC. Letter A shows the location of the start of the plane leg. Letter B shows the location of the end of the plane leg.

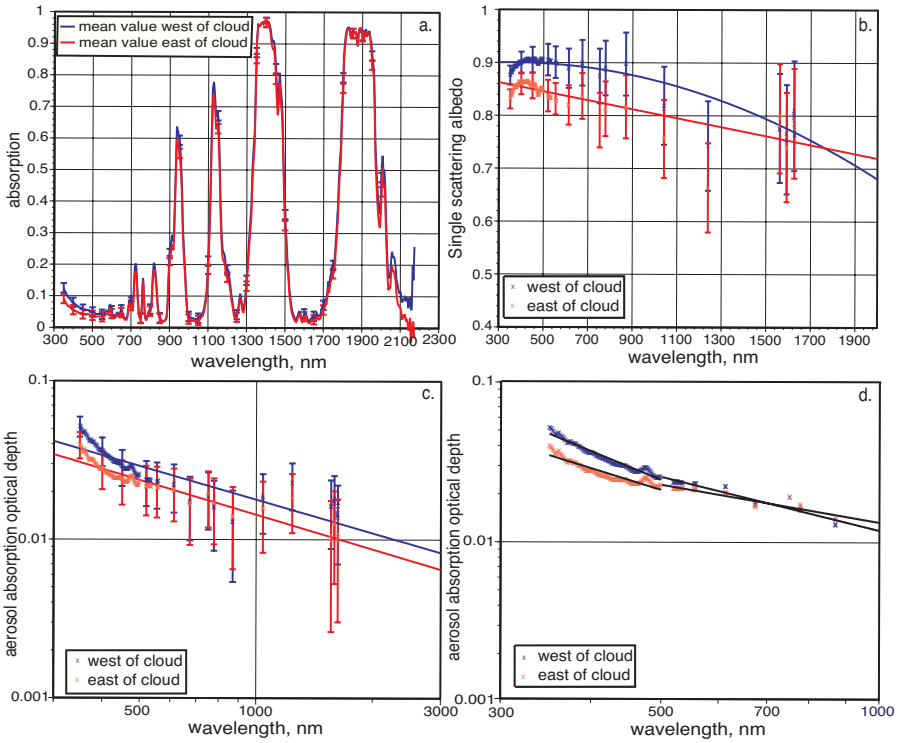

Fig. 3. **(a)** Fractional absorption, **(b)** aerosol single scattering albedo, **(c)** and **(d)** aerosol absorption optical depth for 13 March 2006.

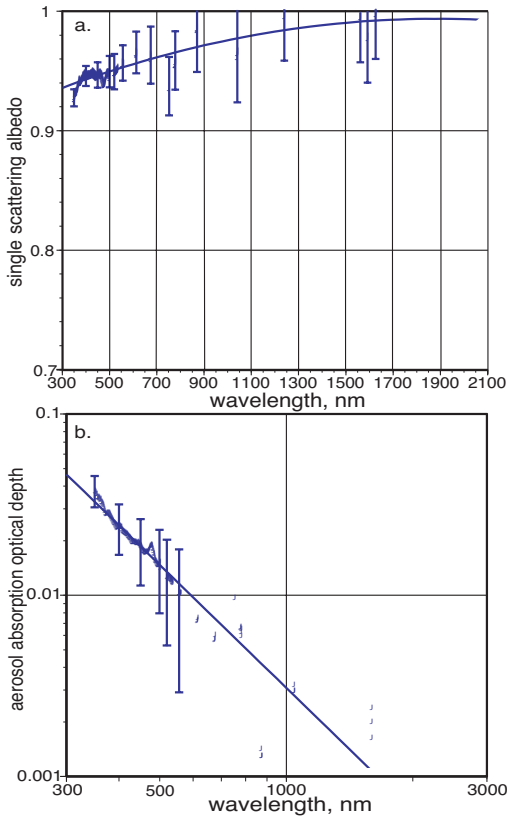

Fig. 4. **(a)** Aerosol single scattering albedo and **(b)** aerosol absorption optical depth for 10 March 2006 (note: for AAOD values below 0.01 the error bars are omitted).

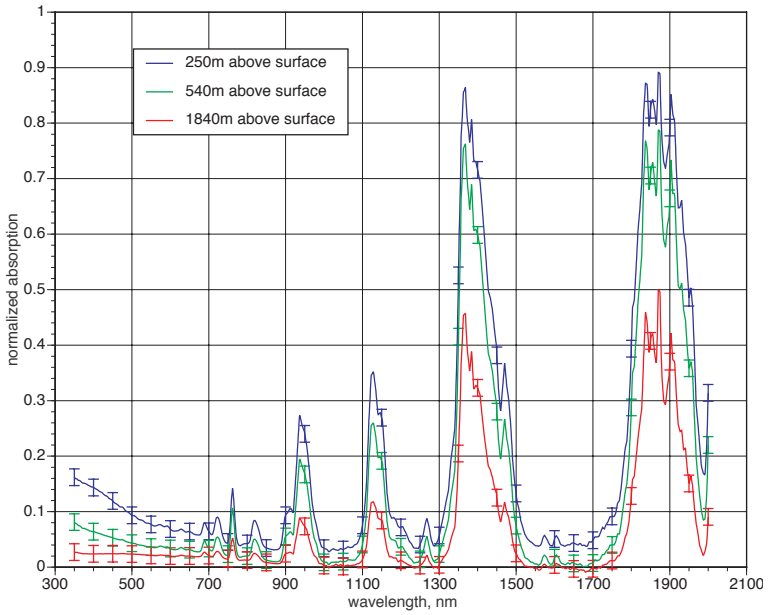

Fig. 5. Fractional absorption at three different altitudes for 6 March 2006.

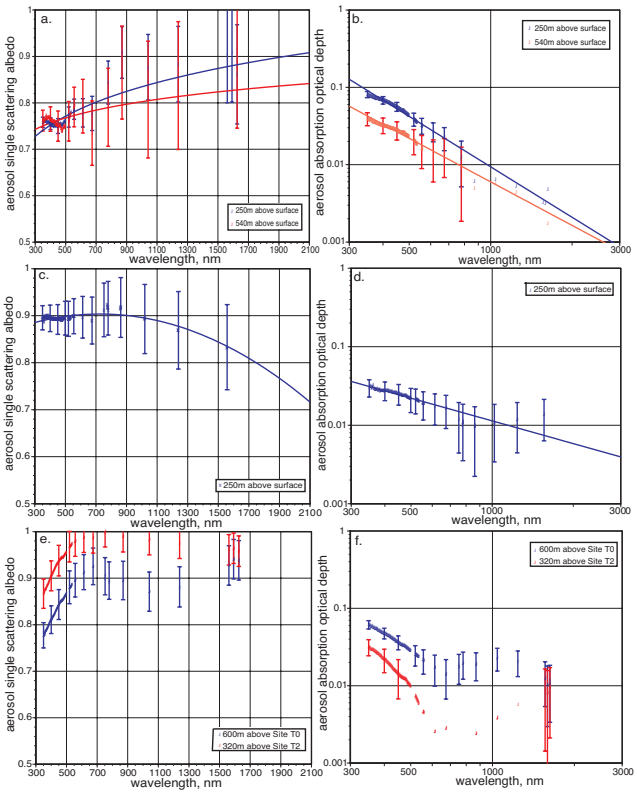

Fig. 6. **(a)** and **(b)**: Aerosol single scattering albedo and absorption optical depth for 6 March 2006. **(c)** and **(d)**: Aerosol single scattering albedo and absorption optical depth for 15 March 2006. **(e)** and **(f)**: Aerosol single scattering albedo and absorption optical depth for 19 March 2006.